

THE LEAD NUCLEUS DISINTEGRATIONS BY 9 GeV PROTONS

BY P. CIOK, J. SIEMIŃSKA

Institute of Nuclear Research, Warsaw*

AND J. WIŚNIEWSKA

Institute of Experimental Physics, University of Warsaw**

(Received February 4, 1974)

The interactions of 9 GeV protons with lead nuclei have been investigated using stacks of nuclear emulsions interlayered with lead foils. The obtained experimental data about the number, nature, and energy of product nuclei have been analysed using the cascade-evaporation model and the radiochemical data for comparison.

1. Introduction

The mechanism of the interaction of high energy particles with heavy nuclei of mass numbers about 200 has been investigated mainly with such experimental methods as radiochemical analysis, counter technique, and mass spectroscopy (see, for example, Refs [1–8]). These methods give rich information on the frequencies of emission of some chosen products and their kinematical characteristics. However, the results obtained in this way concern the characteristics averaged over all the types of interactions. The analysis of individual interactions registered in a track detector can thus provide additional information on the mechanism of the interaction [9].

The experiments performed with the track detector technique, in the above quoted region of target nucleus masses, were concerned until now with special types of interactions or selected products [10–15]. Thus it is desirable to obtain more general information on heavy nucleus disintegrations, particularly with a large number of product nuclei. For this purpose the emulsion technique is particularly useful. In the present work the nuclear emulsions, interlayered with lead foils serving as targets, have been used as detectors of 9 GeV proton-lead nucleus interactions.

* Address: Instytut Badań Jądrowych, Zakład VI, Hoża 69, 00-681 Warszawa, Poland.

** Address: Instytut Fizyki Doświadczalnej, Uniwersytet Warszawski, Hoża 69, 00-681 Warszawa, Poland.

2. The experimental material

Two stacks of nuclear emulsions of different sensitivity, interlayered with lead foils (Fig. 1a), have been irradiated with 9 GeV protons of JINR Synchrotron in Dubna. The emulsion of lower sensitivity (Nikfi-K, sensitive to protons of energies up to 100 MeV) makes it possible to distinguish, by visual estimation of ionisation, between singly and multiply charged nuclei [10]. On the other hand, the electron sensitive emulsion (Nikfi-R) permits to obtain more accurate information about the number of interaction products. The lower intensity of irradiation used in the latter case gives a better scanning efficiency.

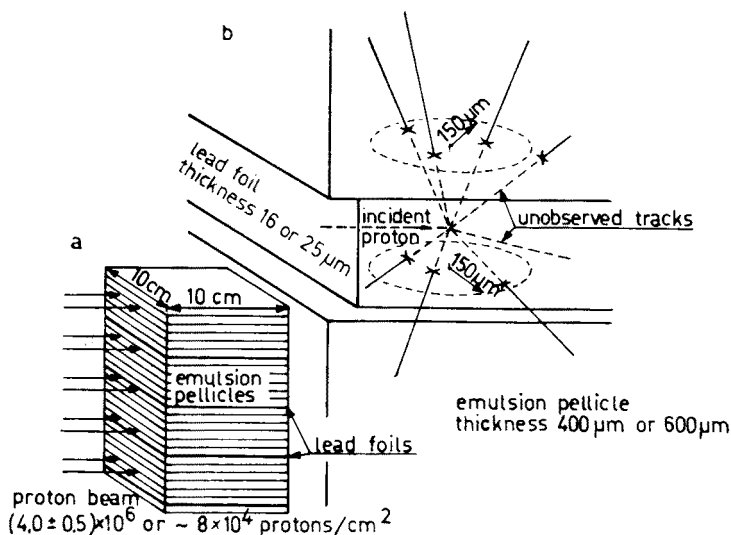


Fig. 1. Illustration of the stack exposure (a) and a proton-lead nucleus interaction recorded in two emulsion layers (b). The first and second sets of numbers correspond to low and electron sensitive emulsion, respectively

Both pellicles neighbouring a lead foil have been independently scanned for at least three tracks appearing to go out from a single point inside the foil, and entering the pellicle in a field of 150 μm radius (Fig. 1b). Each configuration of such tracks in one pellicle was examined in the pellicle on the other side of the foil. In an identified lead nucleus disintegration, only tracks of particles of velocity $v < 0.7c$ have been further taken into account. The number of such particles produced in an interaction is denoted by N_h and corresponds approximately to the number of product nuclei [16]. Depending on the number of these observed tracks in a star, the scanning efficiencies and contributions of secondary interactions¹ have been estimated in both types of emulsion and used afterwards to correct the N_h distribution. In the electron sensitive emulsion a sample of 210 stars with at least four visible tracks of nuclei has been analysed (even in this emulsion the scanning efficiency for smaller stars is less than 50%). In 51 randomly chosen stars the angles of

¹ They have been evaluated using an additional perpendicularly irradiated stack of Nikfi-R emulsions and lead foils.

emission and ranges² (if smaller than 10 mm) of observed product nuclei have been determined.

In the low sensitivity emulsion, a practically unbiased sample of 517 stars with at least nine tracks has been selected for the product identification. (The smaller stars — see Table I — have been treated statistically because of the small scanning efficiency and the large contamination by secondary interactions.) Nuclei with ranges from 0.85 mm to 20 mm, entering the emulsion at angles smaller than 15° , have been identified by the

TABLE I

Some features of analysed interactions of 9 GeV protons with lead nuclei

Emulsion		Electron sensitive	Of low sensitivity
No of interactions	observed	210	635
	corrected	217	624
No of nuclei per interaction	observed	≥ 4	≥ 3
	corrected (N_h)	≥ 5	≥ 5
$\langle N_h \rangle$		20.7 ± 0.7	
cross-section (mb)			1200 ± 180
No of nuclei per interaction	with $R < 5$ mm	13.7 ± 0.5	
	with $Z \geq 2$		5.5 ± 0.2
forward to backward ratio for	all nuclei	1.47 ± 0.05	
	with $R < 5$ mm	1.13 ± 0.08	

range-ionisation method [15]. Moreover for nuclei, entering at any angle into one of the two scanned pellicles and coming to rest in it, the range has been determined and, if possible, the charge numbers $Z = 1$ or $Z \geq 2$ have also been ascribed (in many cases, lithium nuclei and even heavier fragments have been observed).

To each measured track, a geometrical correction has been applied. The number of tracks in a star has been also corrected to the full solid angle. In the case of the low sensitivity emulsion, the loss of about 20% of unrecorded product nuclei was taken into account. The N_h values obtained in this manner do not include tracks shorter than 10 μm because in practice they are not observed. Those tracks correspond to nuclei of very low energy, namely less than about 1 MeV per nucleon.

² By the term "range" we mean the calculated range which a nucleus would have on passing through the emulsion only. The calculation has been done using the range-energy data averaged for protons and deuterons [14, 15].

3. Results and discussion

Lead nucleus disintegrations characterized by the emission of at least five product nuclei of range above $10\ \mu\text{m}$ ($N_h \geq 5$) have been analysed. The cross section for these interactions is equal to $1200 \pm 180\ \text{mb}$. The remaining interactions amount to about 30% of inelastic interactions, however, they contribute less than about 10% to the production of nuclei.

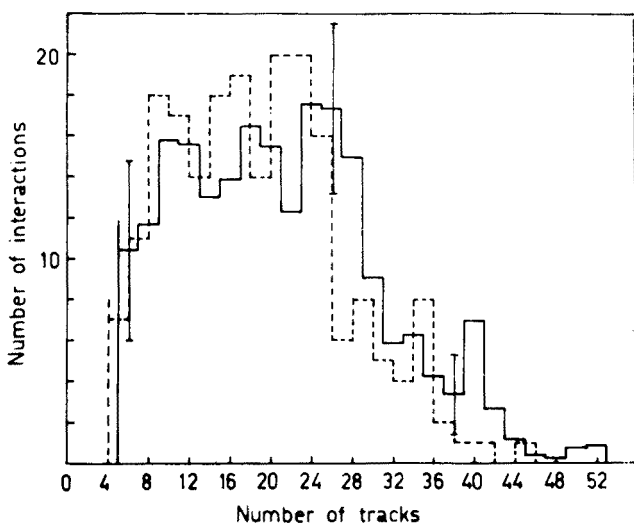


Fig. 2. The distributions of observed (----) and corrected, N_h , (—) numbers of tracks

The N_h distribution (Fig. 2) is almost flat in the region of $N_h \leq 30$. The interactions with $N_h > 30$ amount to about 20% of all analysed interactions. Among them the disintegrations with about 50 product nuclei have been observed. As an example, a star with 46 visible prongs in two pellicles is shown in Fig. 3. The average N_h value is equal to 20.7 ± 0.7 .

Some general features of the analysed interactions and results of measurements are presented in Table I and Figs 4 and 5. The results concerning nuclei with $Z = 1$ and $Z \geq 2$ for stars with medium and large N_h have been extrapolated (taking into account the range distribution given in Fig. 4) into the region of small N_h , for which the ionisation measurements have not been done. The results are given in Table II where the subdivision of multiply charged nuclei based on the data of Goritchev et al. [11] is also presented. The heavy hydrogen isotopes contribute to about 50% of singly charged nuclei [15] and this value only slightly depends on the N_h and on the range in the interval considered (0.85 mm–20 mm).

The observed features of lead disintegration are similar to those of the heavy emulsion nucleus disintegration. Those features are conventionally described by the cascade-evaporation model (see, for example, the classical monograph of Powell et al. [16] and, for new references, the paper of Hyde et al. [8]). So, as the first approximation, we also

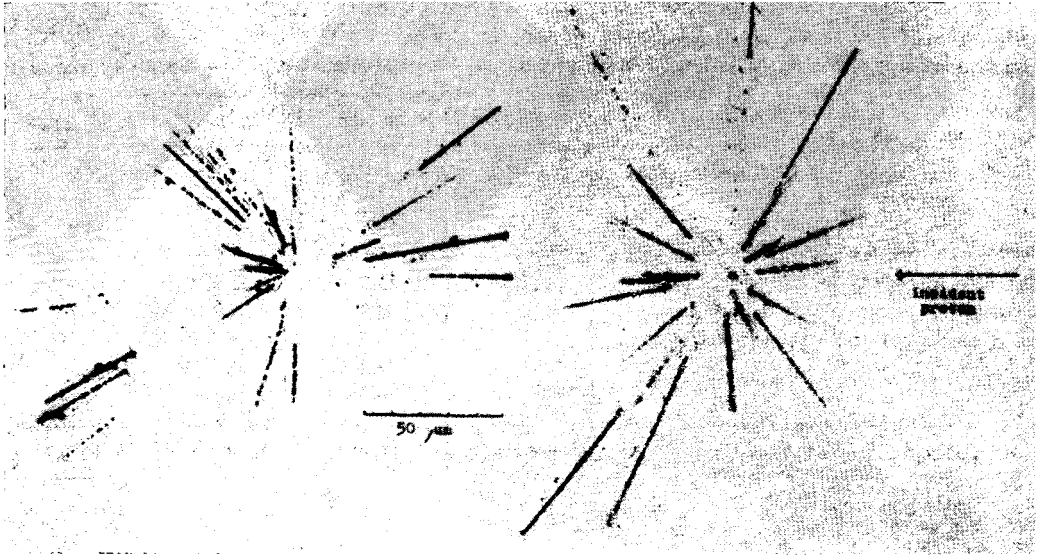


Fig. 3. The microphotograph of a lead nucleus disintegration with 46 visible tracks in two pellicles adjacent to a lead foil

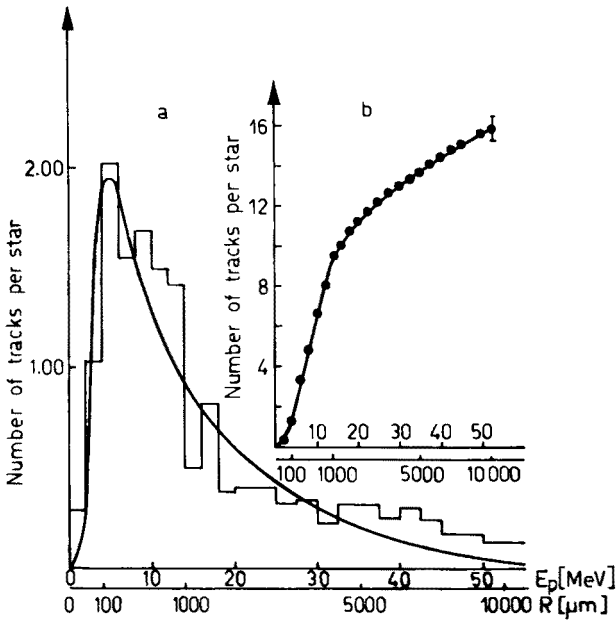


Fig. 4. The differential (a) and integral (b) distributions of ranges of secondary nuclei of interactions with $N_h > 5$, observed in electron sensitive emulsion. The curve in (a) represents the calculated distribution for $T = 10$ MeV

TABLE II

The composition of the nuclei produced in interactions observed in emulsion of low sensitivity (see text)

No of nuclei per interaction	observed	3 – 8	9 – 18	≥ 19	hole sample
	corrected (N_h)	5 – 12	13 – 26	≥ 27	≥ 5
$\langle N_h \rangle$		8.9	20.7	32.1	20.7
No of nuclei per interaction, with charge	1	7.3	15.9	22.6	15.4
	2	1.5	3.9	7.0	4.1
	3	0.1	0.7	1.7	0.8
	4	—	0.2	0.6	0.3
	5	—	0.05	0.2	0.1
$\Delta Z/N_h^*$		1.2 ± 0.1	1.3 ± 0.1	1.4 ± 0.1	1.3 ± 0.1
No of hydrogen nuclei with $R < 5$ mm	p	2.2	4.5	5.9	
	d	2.1	4.5	6.0	
excitation energy U (MeV)		480	840	1230	840

* ΔZ denotes the charge carried out by emitted nuclei

assume that only the process which starts with the cascade and finishes with the evaporation, after which a residual nucleus is left, is responsible for the lead disintegration. We assume, further, that all nuclei with ranges $R > 10 \mu\text{m}$ are the products of evaporation or cascade processes.

The average temperature, T , of emitting nuclei has been estimated as $T = 10 \pm 2$ MeV, by fitting the experimental range distribution (Fig. 5) with the curve evaluated from the evaporation model for the nuclear composition as in Table II. In calculations, the magnitude of the effective potential barrier has been treated as a function of the temperature as suggested by Yamaguchi [19]. The curve for $T = 10$ MeV presented in Fig. 5 is normalized to the experimental histogram in the range interval $0.01 \text{ mm} < R < 5 \text{ mm}$. Nuclei with ranges $R < 5 \text{ mm}$ (corresponding to the proton energy $E_p \leq 35$ MeV) are treated below as evaporated nuclei. They amount to about 67% of all products. About 40% of these nuclei are multiply charged.

The angular distribution of evaporated nuclei gives the average value of the longitudinal velocity, v , of excited nuclei as being in the interval $0.005c - 0.010c$.

Furthermore, the excitation energy, U , of evaporating nuclei and the mass distribution of the residual nuclei have been estimated. The number of evaporated neutrons have been evaluated under the assumption that the neutron to proton ratio for the initial evaporating nuclei is equal to that of lead nuclei, and the residual nuclei with charges $Z_r = 82 - \Delta Z$ have the most probable masses obtained from Ref. [20]. Here ΔZ denotes the charge carried out by N_h products, calculated from a phenomenological formula: $\Delta Z = 1.1 N_h + 0.01 N_h^2$ generalizing the data in Table II. Moreover, calculating the excitation energy, the products with $Z \geq 3$ were regarded as ^8Li nuclei with energies given by Gajewski

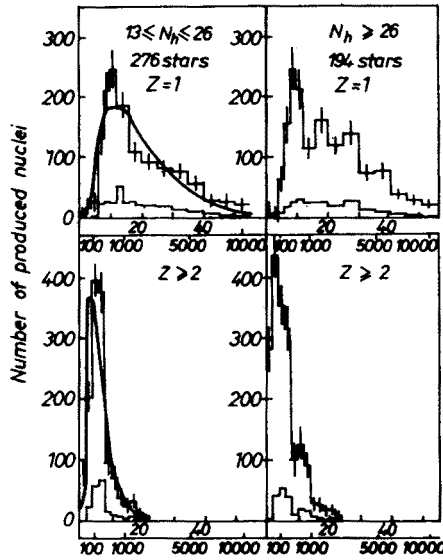


Fig. 5. The range distributions of nuclei with charges $Z = 1$ and $Z \geq 2$ in interactions with medium and large N_h . The indicated curves are calculated for $T = 10$ MeV taking into account the composition of singly and multiply charged nuclei as in Table II

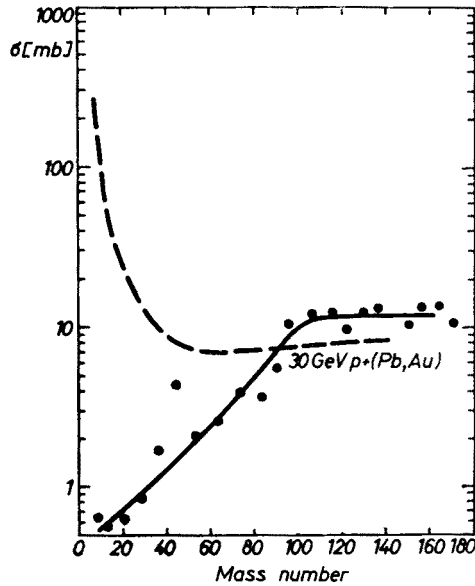


Fig. 6. The residual nucleus mass distribution (—), calculated from the N_h distribution, compared with radiochemical yield-versus-mass curve (---) for 30 GeV proton interaction with Pb and Au nuclei [1]

et al. [10]. The average energy of a single evaporated neutron has been assumed to be half of that of a proton [21]. If the energy of the neutron is higher, for example, equal to the proton energy, the excitation energies given in Table II increase by about 25%.

The residual nucleus mass distribution obtained from the N_h distribution is presented in Fig. 6 together with a radiochemical curve for the interactions of 30 GeV protons³ with Pb and Au nuclei [1]; a marked discrepancy is observed. It must be noted here that the technique applied in this work does not give the possibility of identifying nuclei of short ranges. Moreover, nuclei with ranges $R < 10 \mu\text{m}$ are unobservable, and the production of only one such nucleus in each interaction has been assumed. Calculating the mass of this nucleus, the emission of products solely lighter than carbon has been taken into account (Table II). It is hard to assume that only the emission of heavier nuclei in the cascade-evaporation process, besides the high energy fission [13, 14], with $\sigma_f \approx 120 \text{ mb}$ and the fragment mass distribution in the interval 40 amu — 140 amu [1], can explain such a discrepancy as that observed in Fig. 6 above the boron mass. Other processes can contribute here, for example, the rapid break-up of a nucleus, considered in the bromium and silver fragmentation [22, 23], can play even more important role in lead disintegrations.

We wish to express our gratitude to Professor J. Zakrzewski, Professor P. Zieliński and Dr M. Świącki for their help and valuable advices. We thank the team of physicists of the JINR in Dubna for the irradiation and processing of the stacks, and also the scanning team in Warsaw for careful scanning and measurements.

REFERENCES

- [1] J. Hudis, T. Kirsten, R. W. Stoenner, O. A. Schaeffer, *Phys. Rev.* **C1**, 2019 (1970).
- [2] L. P. Remsberg, F. Plasil, J. B. Cumming, M. L. Perlman, *Phys. Rev.* **C1**, 265 (1970).
- [3] K. Beg, N. T. Porile, *Phys. Rev.* **C3**, 1631 (1971).
- [4] A. M. Poskanzer, G. W. Butler, E. K. Hyde, *Phys. Rev.* **C3**, 882 (1971).
- [5] Y. Y. Chu, S. M. Franz, G. Friedlander, P. J. Karol, *Phys. Rev.* **C4**, 2202 (1971).
- [6] E. K. Hyde, G. W. Butler, A. M. Poskanzer, *Phys. Rev.* **C4**, 1759 (1971).
- [7] J. B. Cumming, K. Bächmann, *Phys. Rev.* **C6**, 1362 (1972).
- [8] R. G. Korteling, C. R. Toren, E. K. Hyde, *Phys. Rev.* **C7**, 1611 (1973).
- [9] G. Rudstam, S. O. Sörensen, *J. Inorg. Nucl. Chem.* **28**, 771 (1966).
- [10] W. Gajewski, P. A. Goritchev, N. A. Perfilov, *Nucl. Phys.* **69**, 445 (1963).
- [11] P. A. Goritchev, O. V. Lozhkin, N. A. Perfilov, *Yad. Fiz.* **5**, 26 (1967).
- [12] J. Hudis, S. Katcoff, *Phys. Rev.* **180**, 1122 (1969).
- [13] G. Remy, J. Ralarosy, R. Stein, M. Debeauvais, J. Tripier, *Nucl. Phys.* **A163**, 583 (1971).
- [14] R. Brandt, F. Carbonara, E. Cieślak, H. Piekarz, J. Piekarz, J. Zakrzewski, *Rev. Phys. Appl.* **2**, 243 (1972).
- [15] P. Ciok, Report of Inst. of Nucl. Research, Warsaw 1256/VI/PL.
- [16] C. F. Powell, P. H. Fowler, D. H. Perkins, *The Study of Elementary Particles by the Photographic Method*, Pergamon Press (1959) p. 423.

³ In spite of the difference in the incident proton energies, the comparison of both curves is justified because the interaction features we are interested in are nearly independent of the primary proton energy above about 6 GeV [1].

- [17] C. F. Williamson, J. P. Boujot, J. Picard, Report CEA-R 3042 (1966).
- [18] W. R. Barkas, UCRL 8763 (1959).
- [19] Y. Yamaguchi, *Prog. Theor. Phys.* **5**, 501 (1950).
- [20] G. Friedlander, in *Proceedings of the Symposium on the Physics and Chemistry of Fission, Salzburg, Austria*, 1965 (IAEA, Vienna, Austria) Vol. II, p. 265.
- [21] I. Dostrovsky, R. Bivins, P. Rabinowitz, *Phys. Rev.* **111**, 1659 (1958).
- [22] E. Makowska, J. Siemińska, J. Suchorzewska, *Acta Phys. Pol.* **33**, 105 (1968).
- [23] K. D. Tolstov, R. A. Khoshmukhamsdov, Report of JINR, Dubna P1-6897 (1973).